Life Sciences 227 (2019) 39–50

Contents lists available at ScienceDirect

Life Sciences

journal homepage: www.elsevier.com/locate/lifescie

New folate receptor targeted nano liposomes for delivery of 5-fluorouracil to cancer cells: Strong implication for enhanced potency and safety

Somayeh Handali[a], Eskandar Moghimipour[a,b], Maryam Kouchak[a], Zahra Ramezani[a], Mohsen Amini[c], Kambiz Ahmadi Angali[d], Sadegh Saremy[b], Farid Abedin Dorkoosh[e,f], Mohsen Rezaei[g,*]

[a] Nanotechnology Research Center, Ahvaz Jundishapur University of Medical Sciences, Ahvaz, Iran
[b] Cellular and Molecular Research Center, Ahvaz Jundishapur University of Medical Sciences, Ahvaz, Iran
[c] Department of Medicinal Chemistry, Faculty of Pharmacy, Tehran University of Medical Sciences, Tehran, Iran
[d] Department of Biostatistics, School of Public Health, Ahvaz Jundishapur University of Medical Sciences, Ahvaz, Iran
[e] Department of Pharmaceutics, Faculty of Pharmacy, Tehran University of Medical Sciences, Tehran, Iran
[f] Medical Biomaterial Research Centre (MBRC), Tehran University of Medical Sciences, Tehran, Iran
[g] Department of Toxicology, Faculty of Medical Sciences, Tarbiat Modares University, Tehran, Iran

ARTICLE INFO

Keywords:
Liposome
Response surface methodology
5-Fluorouracil
Folic acid
Targeted drug delivery

ABSTRACT

We previously showed that folate liposomes of 5FU made from Dipalmitoylphosphatidylcholine (DPPC) induced cell death in HT-29 and HeLa cells more potently than bulk 5FU. Also, a primary 5FU liposomal formulation with phosphatidyl choline (PC) exhibited higher cytotoxicity in murine colon cancer cells. In the present study, optimization of 5FU PC liposome, mechanism of cell death induction in human cancer cell lines and its safety along with other assays have been employed for targeted PC liposomes of 5FU.

Liposomes were prepared using thin layer method and optimization of preparation was assessed using central composite design (CCD) of response surface methodology (RSM). Folic acid (FA) was employed as the targeting ligand. Morphology of 5FU loaded liposomes and changes in their thermal behavior were assessed by transmission electron microscopy (TEM) and differential scanning calorimetry (DSC), respectively. *In vitro* cytotoxicity was explored using MTT assay in HT-29, Caco-2, HeLa and MCF-7 cell lines. Cytotoxicity mechanism of the targeted delivery system was searched through the evaluation of reactive oxygen species (ROS) overproduction, mitochondrial membrane potential ($\Delta\Psi_m$), the release of cytochrome *c*, the activity of caspase 3/7 and apoptosis and necrosis rate. Liposomes were spherical in shape and 5FU was successfully encapsulated into liposomes rather in an amorphous state. Our interesting results showed that in HT-29 cells targeted liposomes triggered the mitochondrial apoptotic pathway by decreasing the mitochondrial membrane potential, releasing of cytochrome *c* and promoting the substantial activity of caspase 3/7. In HeLa cells, however, targeted liposomes particularly activated necrosis pathway through the overproduction of ROS. Folate-liposomal 5FU showed significantly higher antitumor efficiency compared to free drug. The results of this study offer new prospects for cancer therapy with reducing systemic drug exposure and associated toxicities.

1. Introduction

5-Fluorouracil (5FU) is a pyrimidine analogue and one of the most widely used agents in the first-line chemotherapy for colon cancer. Its mechanism of action is mainly through the inhibition of RNA function or processing and synthesis of thymidylate [1,2]. In order to attain its therapeutic level, 5FU is administered at relatively high doses (400–600 mg/m^2). Nevertheless, due to the short half-life of 15–20 min, tumor cells are only exposed to a narrow concentration of active metabolite during an insufficient time [3]. Moreover, clinical use of 5FU is restricted because severe systemic toxic effects including hematologic, gastrointestinal, neural, cardiac and dermatologic toxicities would occur upon its intravenous administration [4]. Through oral administration, bioavailability of 5FU was reported to be 28% in human [2].

Targeted or smart drug delivery systems have provided valuable facilities for lowering of adverse drug effects *via* the liberation of appropriate amount of drug in a targeted tissue. Loading of 5FU to a nano-

* Corresponding author at: Department of Toxicology, Faculty of Medical Sciences, Tarbiat Modares University, Tehran, P.O. Box: 14115-331, Iran.
E-mail address: rezaei.mohsen@gmail.com (M. Rezaei).

https://doi.org/10.1016/j.lfs.2019.04.030
Received 17 March 2019; Received in revised form 8 April 2019; Accepted 14 April 2019
Available online 16 April 2019
0024-3205/

platform will not only reduce its systemic toxicity but also will provide more desired action [1] by reducing the dose and duration of therapy [5]. In order to selectively deliver chemotherapeutic drugs to cancer cells various targeting molecules such as antibodies, cytokines, peptides, growth factors, polysaccharides, and folic acid (FA) could be conjugated to the surface of the nano-particles. Targeted cancer therapy allows the exposure of cancer cells to the cytotoxic drug while restricting the exposure of normal cells [6]. Given that it is small, non-toxic, non-immunogenic, inexpensive and stable in storage and in circulation, folic acid offers several advantages as a targeting tool over others [7,8].

Liposomes are nano-sized spherical vesicles composed of one or several concentric phospholipid bilayers with an internal aqueous phase. Due to their specific structure, they can be used for encapsulation of both water-soluble and lipophilic drugs [9,10]. Liposomes were extensively used as drug delivery system for a wide range of drugs with different physicochemical properties [11]. Owing to their biocompatibility, biodegradability and higher safety [12–14], they can improve the therapeutic activity and specificity of drugs [10]. A significant limitation in developing of liposome based formulations for hydrophilic molecules like 5FU is the modest efficiency in encapsulation process mainly due to its high aqueous solubility.

Estimation of the amount of drug encapsulated in liposomes is complicated and it is dependent on many parameters such as preparation procedure, lipid concentration and liposomal particle size [15]. Response surface methodology (RSM) is a rapid statistical method through which quantitative data from appropriate experiments apply to fit regression model equations and operating conditions [16,17]. The technique is less time-consuming than other approaches due to reducing the number of experimental runs. RSM can not only reveal the relationship between the response and the independent variables, but also take interaction effects of the variables into consideration [18]. In addition, it determines the optimum level of experimental parameters required for given responses [17]. RSM has been extensively applied to pharmaceutical systems, including the preparation of nano-drug delivery formulations [12]. Central composite design (CCD) is a usual experimental design used in RSM for liposome formulation optimization to evaluate various factors including the factors which affect entrapment efficiency (EE) of the drug [19–21]. One of the advantages of CCD is to reduce the number of experiments in the studies with a large number of variables and levels [20].

The mechanism of action of various anticancer drugs has been studied. Many of anti-cancer drugs induce cell death by apoptosis and/or necrosis. Mitochondrion is one of the most important organelle for apoptosis induction in cancer cells and anticancer drugs affect mitochondria through several critical signaling pathways in cancer cells. Enhancing the sensitization of cancer cells to drug-induced apoptosis has become an important strategy for antitumor drugs. Using of targeted formulations could alter the amount of drug in contact with intracellular and extracellular milieu of cancer cells. This approach may affect cell organelles such as mitochondria in a way different from conventional formulations which can potentially be developed for clinical therapy of cancer.

The aim of this study was to introduce an efficient encapsulation procedure for preparation and optimization of targeted 5FU contained nano-liposomes. Also, in this study we tested whether the modification of formulation in this way could alter the mechanism by which 5FU exerts its toxic effect on cancerous and normal cells.

2. Materials and methods

5Fluorouracil (5FU) and soya phosphatidyl choline (PC) were obtained from Acros, USA. Cholesterol was purchased from Merck, Germany. Metronidazole was kindly donated by Pars Darou Pharmaceutical Co., Iran. Distearoylphosphatidylethanolamine (DSPE) was acquired from Lipoid, Germany. Sucrose, folic acid (FA) and poly (ethylene glycol) 2-aminoethyl ether acetic acid (NH_2-PEG-COOH) were obtained from Sigma-Aldrich, Germany. *N*-Hydroxysuccinimide (NHS) and triethylamine (TEA) were purchased from Merck, Germany. 1-Ethyl-3-(3-dimethylaminopropyl) carbodiimide (EDC) was acquired from Alfa Aesar, Germany. Dialysis membrane (Spectra/Por®) was purchased from Biotech, USA.

HT-29 (human colorectal adenocarcinoma), Caco-2 (human colon adenocarcinoma), MCF-7 (human breast adenocarcinoma cell line) and fibroblast (Hu02) cells were obtained from Iranian Biological Resource Center (IBRC). HeLa (human cervix carcinoma cell line) and CT26 (murine colon carcinoma) were purchased from National Cell Bank of Iran (NCBI), Pastor Institute, Iran. 3-(4, 5-dimethyl-2-thiazolyl)-2, 5-diphenyl tetrazolium bromide (MTT) and Dulbecco's modified eagle's medium (DMEM) and fetal bovine serum (FBS) was purchased from Gibco, USA. Penicillin-streptomycin was acquired from Sigma-Aldrich, Germany. 2′,7′-Dichlorofluorescin diacetate (DCFDA) was purchased from Sigma-Aldrich, Germany. MitoLight™ Apoptosis Detection Kit was obtained from Merck Millipore, USA. Cytochrome c human ELISA kit was provided from Abcam, USA. Caspase-Glo® 3/7 kit was acquired from Promega, USA and Annexin V-FITC apoptosis detection kit was purchased from Sigma Aldrich, USA. BALB/c mice were obtained from the Pasteur Institute of Iran. All of the solvents were of the analytical grade.

2.1. Experimental design

CDD response surface methodology was selected in order to investigate the effect of quantitative independent variables including amounts of 5FU (*X1*) and PC (*X2*) on the physicochemical properties of the drug loaded liposome. The total phospholipids and cholesterol contents were kept constant in all formulations (10 mg and 1 mol, respectively). Dependent variables were encapsulation efficiency (EE%) of 5FU (*Y1*) and liposome size (PZ) (*Y2*). The variables and their levels are tabulated in Table 1. The selection of the low and high values was based on the pilot study results. Data were fitted by Design-Expert® software (version 7.0.0, stat-Ease, Inc., Minneapolis, MN) and the tridimensional response surfaces and contour plots were generated to demonstrate any relationship between the response and experimental levels of each factor [22]. Based on this software, performing a total of 10 runs was required to develop appropriate models. Significant differences of the variables of the responses were achieved by ANOVA test (p-value < 0.05). The preferred characteristics of the responses were the smaller liposome size and higher encapsulation efficiencies of the drug. The optimized predicted formulation was prepared in triplicate and the actual results were compared to the predicted ones.

2.2. Synthesis of Folate-PEG-DSPE

Folate-PEG-DSPE was synthesized as explained previously [23]. Briefly, Folic acid dissolved in methanol containing TEA and the reaction started by addition of EDC. One h later, NHS was added and stirred for 4 h. The activated folic acid was then reacted with NH_2-PEG-COOH

Table 1
Variables used in CDD response surface design.

Independent variables	Factors	Units	Type	Levels	
				Low	High
X_1	Drug	mg/mL	Numerical	1.87	4.37
X_2	PC	mole/mL	Numerical	0.5	2

Dependent variables	Units	Constrains
Y_1 = EE %	%	Maximum
Y_2 = Size	nm	Minimum

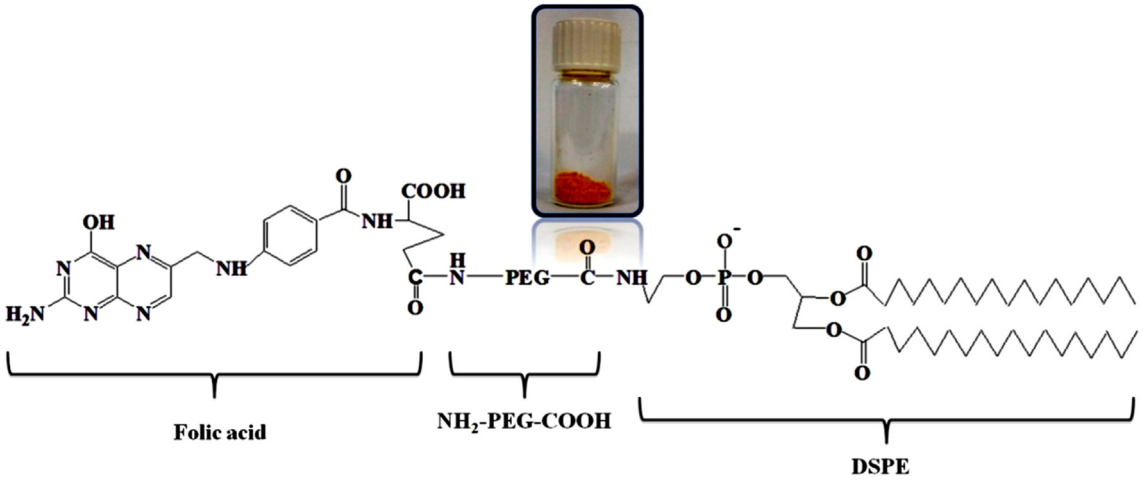

Fig. 1. FA-PEG-DSPE.

at room temperature for 48 h. Solvent was evaporated from the reaction mixture and the remained yellow color product suspended in deionized water. The resultant suspension was dialyzed against deionized water three times using dialysis membrane (MWCO 1000 Da) and the final product (FA-PEG-COOH) was then freeze-dried. For preparing of FA-PEG-DSPE, FA-PEG-COOH was activated and reacted with the amine group of DSPE. Briefly, FA-PEG-COOH dissolved in methanol containing TEA and incubated for 1 h with EDC at room temperature. NHS was added and the mixture stirred for 3 h prior to adding DSPE. The mixture was shaken over night at room temperature and dialyzed against deionized water, freeze-dried under vacuum to obtain FA-PEG-DSPE conjugate (Fig. 1). Conjugates were confirmed by ^{1}H NMR spectroscopy (500 MHz, Bruker, Germany).

2.3. Preparation of liposomes

Liposomes were prepared using thin film method. At first optimized combination of concentration of PC and 5FU were calculated and experimented carefully (details were mentioned in experimental design section). PC, cholesterol and FA-PEG-DSPE were dissolved in chloroform in different molar ratios as described in the Table 1. The solvent was removed by rotary evaporator under vacuum (Heidolph, Germany). Lipid layer was hydrated with phosphate buffer saline (PBS) (pH 7.4) containing 5FU in different concentrations. The suspension was sonicated for 5 min and then homogenized for 5 additional min. Suspension stored for 24 h in refrigerator (4 °C) and unentrapped 5FU was removed from the liposome dispersions by centrifugation at 15000 rpm for 30 min (MPW-350R, Poland). The liposome pellet was resuspended in PBS containing sucrose as cryoprotectant and then freeze dried. To maintain the similar particle size distribution and to avoid leakage of the encapsulated drug from liposomes during freeze-drying, different molar ratios of sucrose to lipid (0.5:1, 1:1, 2:1) were investigated for 3 months.

2.4. Particle size determination

The average diameter of liposomes was determined using a particle sizer (Qudix, ScatterOScope I, Korea) system at 25 °C. Liposomal suspensions were diluted with deionized water before the measurement.

2.5. Evaluation of encapsulation efficiency

The liposomal suspension centrifuged at 15000 rpm for 30 min and the supernatant analyzed using HPLC (Waters, USA). Metronidazole was applied as internal standard. The HPLC system equipped with Waters 1525 binary Pump and C_{18} column (250 × 4 mm i.d., 5 μm) was used. The mobile phase was composed of 0.02 M phosphate buffer (pH 4) and methanol (70:30, V/V). The filtered mobile phase was pumped at flow rate of 0.8 mL/min and the column temperature was maintained at 30 °C. The eluent was detected by UV detector at 260 nm and injection volume was 50 μL. Formula (1) was employed to calculate the encapsulation efficiency (EE%) of liposomes:

$$\text{Encapsulation Efficiency (EE\%)} = (W_i - W_e/W_i) \times 100 \quad (1)$$

where W_e is the amount of remained free 5FU in supernatant and W_i is the initial amount of the drug.

2.6. Differential scanning calorimetry (DSC)

Thermal analysis of 5FU liposomes were performed using a differential scanning calorimeter (DSC-1 Mettler Toledo, Switzerland). DSC measurements were also carried out for 5FU, PC, cholesterol individually, the physical mixture of the formulation components and freeze dried 5FU loaded liposome to evaluate any changes during formulation preparation. About 5 mg of each agent was weighed, crimped into an aluminum pan and analyzed at a temperature range from 0 to 300 °C for 30 min.

2.7. Transmission electron microscopy (TEM)

The morphology of liposomes was visualized by transmission electron microscopy (Philips, CM 30, Eindhoven, The Netherlands). Samples were diluted with deionized water and one drop of the liposomal formulation was placed on a carbon-coated copper grid and air-dried at room temperature. Then, samples were stained with 1% uranyl acetate for viewing.

2.8. Cytotoxicity assay

Cell viability was evaluated using MTT assay. This assay is based on the cleavage of yellow tetrazolium salt MTT by mitochondrial enzymes, mainly by succinate dehydrogenase to form a dark blue crystalline product, formazan [24,25]. HT-29 and Caco-2 (colon cancer cell lines), HeLa (folate receptor positive), MCF-7 (folate receptor negative) and fibroblast (normal cell) were grown at 37 °C, 5% CO_2 and 95% relative humidity in DMEM supplemented with 10% FBS and 1% penicillin-streptomycin. After overnight incubation, cells were seeded at a density of 1 × 10^4 cells in 96-well culture plates and incubated for 24 h at 37 °C. Then, cells were treated with different concentrations of 5FU, liposomal 5FU and folate-liposomal 5FU (25, 35, 50, 75 and 100 μM) for 48 h. After 48 h, 20 μL of MTT (5 mg/mL in PBS) solution was added into each well and incubated for 4 h. Afterwards, 150 μL of dimethyl

sulphoxide (DMSO) was added to each well and the plates were mildly shaken for 20 min. Cell viability was recorded at 570 nm using ELISA plate reader (BioRad, USA). The survival rates were calculated using the formula (2):

$$\text{Cell viability\%} = (\text{Abs}_{\text{sample}}/\text{Abs}_{\text{control}}) \times 100 \quad (2)$$

Note: MTT assay reveled that there is no significant difference between 5FU and liposomal 5FU in cell viability in all cell lines. So, further evaluations as outlined below were only performed for 5FU and folate-liposomal 5FU at their IC_{50} concentrations.

2.9. Measurement of reactive oxygen species (ROS)

Generation of ROS was evaluated using 2′,7′-dichlorofluorescin diacetate (DCFDA), which is a non-fluorescent molecule that passively diffuses into cells. After diffusing into cells, DCFDA is deacetylated by cellular esterases to a non-fluorescent compound, which gets rapidly oxidized to the highly fluorescent 2, 7-dichlorofluorescein (DCF) in the presence of intracellular ROS [26]. Cells at 1×10^5 were seeded into 6-well plate and allowed to attach for 24 h. Then, the wells were treated with free 5FU and folate-liposomal 5FU for 1, 3 and 48 h. The cells were then washed with PBS and DCFDA (10 μM) added and incubated for 45 min at 37 °C. Fluorescence was recorded at excitation wavelength of 485 nm and emission wavelength of 530 nm using spectrofluorimeter (PerkinElmer, USA).

2.10. Mitochondrial transmembrane potential ($\Delta\Psi_m$) analysis

$\Delta\Psi_m$ was measured using MitoLight™ Apoptosis Detection Kit (Merck Millipore, USA). Briefly, cells were treated with 5FU and folate-liposomal 5FU for 48 h. Then cells were incubated with MitoLight™ solution for 20 min at 37 °C and were re-suspended in incubation buffer and analyzed using flow cytometer (Facs Calibur, BD, USA).

2.11. Release of cytochrome c from mitochondria

Release of cytochrome *c* from mitochondria was detected using cytochrome *c* human ELISA kit according to the manufacturer's instructions (abcam, USA). Briefly, cells were treated with 5FU and folate-liposomal 5FU for 48 h. Then samples were added to the microplates and 50 μL of antibody was added to all wells and incubated at room temperature for 2 h. 100 μL of streptavidin HRP-solution was added and incubated at room temperature for 1 h. Then, 100 μL of TMB solution was pipetted into each well. Finally, the enzyme reaction was stopped by adding 100 μL of stop solution and cytochrome *c* release was assessed by measuring absorbance at 450 nm using an ELISA plate reader (BioRad, USA).

2.12. Caspase activity

Caspase-3/7 activity was evaluated using the Caspase-Glo® 3/7 Assay (Promega, USA) according to the kit instructions. Cells were seeded in 96-well plates for 24 h. Following incubation overnight, cells were treated with free 5FU and folate-liposomal 5FU for 48 h. After incubation, plates were removed from the incubator and allowed to equilibrate to room temperature. Then, 100 μL of Caspase-Glo® 3/7 reagent was added to each well. Contents of wells was gently mixed using a plate shaker at 300–500 rpm for 30s and incubated at room temperature for 30 min to 3 h. Luminescence was measured subsequently (Titertek-Berthold, Germany).

2.13. Determination of apoptosis

The apoptosis rate was measured using Annexin V-FITC apoptosis detection kit according to the manufacturer's instructions (Sigma Aldrich, USA). Briefly, HT-29 and HeLa cells were seeded into 6-well culture plates at a density of 1×10^6 cells/well. After 24 h incubation, they were treated with 5FU and folate-liposomal 5FU for 48 h and suspended in the binding buffer and then 5 μL of Annexin V-FITC and 10 μL of Propidium Iodide (PI) were added into the suspensions. The suspensions were incubated at room temperature in the dark for 10 min. The apoptosis rates were measured using a flow cytometer (Facs Calibur, BD, USA).

2.14. In Vivo antitumor effect and histopathological study

The animal protocols were performed according to the guidelines of the Animal Ethics Committee Jundishapur University of Medical Sciences, Ahvaz, Iran with reference number: IR.AJUMS.REC.1395.643. The subcutaneous tumors in BALB/c male mice were inoculated with 100 μL of cell suspension containing 1×10^6 CT26 cell. Tumors were allowed to grow at 100 mm^3 and the mice were randomly divided into three groups, each group having three mice: (1) control, (2) 5FU and (3) folate-liposomal 5FU. The intraperitoneally formulation dose was equivalent to 20 mg/kg 5FU injected every other day (5 injections for period of 13 days) and tumor volume was measured by a caliper and calculated using the Eq. (3):

$$V = (W^2 \times L)/2 \quad (3)$$

where L and W are is the longest and shortest diameter, respectively. Also, body weight, movement and feeding were evaluated during the experiment. At the end of treatment (day 21), mice were sacrificed and tumors were excised and fixed with 10% paraformaldehyde, embedded in paraffin and sectioned. The tissue slices were strained with hematoxylin and eosin (H&E) and observed using optical microscope (Olympus IX50, Japan).

3. Results

RSM is an effective statistical technique used to evaluate multiple parameters and their interactions in formulation design [17]. CCD which is one of the common experimental design method used in RSM evaluation [20,21] employed to obtain the exact relationship between factors for finding the optimal response. The values of independent variables and the related experimental data in 10 suggested formulations based on CDD design have been summarized in Table 2.

The analysis of variance for EE% as a response is shown in Table 3. Consequently, a quadratic second-order polynomial Eq. (4) was fitted as below:

$$Y_1 = +131.80759 - 63.23123\,(X_1) - 50.21197\,(X_2) - 1.43250\,(X_1)\,(X_2) + 11.74683\,(X_1)^2 + 24.08560\,(X_2)^2 \quad (4)$$

where Y_1 is the predicted EE% and X_1 and X_2 are the amounts of 5FU and PC, respectively. As illustrated in the Table 3, the lack of fit of the obtained equation is not significant (*F*-value = 0.74). Also, for the good fit of a model coefficient of determination (R^2) should be 0.80 or higher

Table 2
CDD experimental runs and corresponded responses.

Run no.	Independent variables		Dependent variables	
	X_1	X_2	Y_1` (EE%)	Y_2 (nm)
1	3.50	2.00	45.0451	136
2	2.50	1.25	13.3836	147
3	2.50	2.31	46.234	117.333
4	3.50	0.50	32.2692	186.333
5	2.50	0.19	40.0996	172.333
6	1.09	1.25	49.3637	101.8
7	1.50	0.50	41.4127	178.667
8	2.50	1.25	21.6952	135.667
9	3.91	1.25	29.7646	182
10	1.50	2.00	58.4861	101.55

Table 3
The analysis of variances for EE% as the response (Y_1).

Source	Sum of squares	df	Mean squares	*F*-value	*p*-Value*
Model	1543.14	5	308.63	11.11	0.0184
X_1	316.28	1	316.28	11.38	0.0279
X_2	185.52	1	185.52	6.68	0.0611
X_1X_2	4.62	1	4.62	0.17	0.7044
X_1^2	630.80	1	630.80	22.70	0.0089
X_2^2	839.10	1	839.10	30.20	0.0053
Residual	111.14	4	27.78		
Lack of fit	76.60	3	25.53	0.74	0.6711
Pure error	34.54	1	34.54		
Cor. total	1654.27	9			
R^2	0.9328				
Adjusted R^2	0.8488				

* Significant at 0.05 level.

which implies an optimum adequacy of the applied regression model [16]. In this study, the coefficient of determination (R^2) and adjusted R^2 of this model were predicted to be 0.93 and 0.84, respectively. This coefficient of determination (R^2) explains 93% of response variabilities by the model. The proximity between R^2 and adjusted R^2 demonstrated the efficiency of the model to predict the response (EE %) by the optimized method.

Table 4 shows the analysis of variance for the regression coefficients of particle size as a response of independent variables. Insignificant lack of fit ($F = 3.35$; p value = 0.3957) represent that a linear model is the best fitted model for particle size with the following Eq. (5):

$$Y_2 = +140.01994 + 19.44199\,(X_1) - 34.20529\,(X_2) \quad (5)$$

where Y_2 is the particle size and X_1 and X_2 are the amounts of 5FU and PC, respectively. The coefficient of determination (R^2) and adjusted R^2 of this model were predicted to be 0.85 and 0.81, respectively. Low p-value ($p < 0.001$) confirmed that the model can significantly represent the actual relationship between parameters and response.

The 3D response surface plot of EE% and particle size of liposomes is illustrated in Fig. 2. According to this fig, EE% increased parallel to enhancement of the amount of PC. On the other hand, the EE% decreased by increasing the amount of 5FU. As shown in Fig. 2, by increasing 5FU, particle size of liposomes was enhanced, while PC increasing made it was declined.

3.1. Optimization and validation of model

For model validation and determination of prediction error, the liposomes were prepared and characterized using the selected optimal conditions ($n = 3$). The observed responses followed by predicated error values were indicated in Table 5. According to the results, there is a reasonable correlation between the predicted and observed amounts for the liposome size and EE%, which shows significance adequacy and predictability of models.

Table 4
The analysis of variances for liposome size as the response (Y_2).

Source	Sum of squares	df	Mean squares	*F*-value	*p*-Value*
Model	8288.94	2	4144.47	21.44	0.0010
X_1	3023.93	1	3023.93	15.64	0.0055
X_2	5265.01	1	5265.01	27.24	0.0012
Residual	1353.21	7	193.32		
Lack of fit	1288.99	6	214.83	3.35	0.3957
Pure error	64.22	1	64.22		
Cor. total	9642.15	9			
R^2	0.8597				
Adjusted R^2	0.8196				

* Significant at 0.05 level.

3.2. DSC analysis

DSC is a very useful tool, which can be used to investigate the interaction between liposomes and drug molecules [27] and provide information about the physicochemical state of drug while inside the drug delivery systems [28]. Thermogram of 5FU, cholesterol, PC, physical mixture of 5FU/cholesterol/PC, 5FU loaded liposome and freeze dried powder of 5FU loaded liposome are illustrated in Fig. 3A(a–e). The DSC curve of 5FU exhibits a sharp endothermic peak at temperature of 282 °C corresponding to its melting point (Fig. 3Aa), which is in agreement with the previous reports [29–31]. This peak is also detected in the thermogram of the physical mixture 5FU/cholesterol/PC, although the peak becomes less intensive and the temperature of peak shifts towards lower temperature (280 °C), while no endothermic peak is found in the drug loaded liposome and freeze dried powder of 5FU loaded liposome, which demonstrates that 5FU exists in amorphous phase in the liposome.

3.3. Transmission electron microscopy (TEM)

As shown in Fig. 3B, liposomes are spherical in shape with bilayer lipid membrane and nanometric-size range. Liposomal particle size was in correlation with the measured values obtained from dynamic light scattering method.

3.4. Freeze-drying of liposomes

Freeze drying is potentially detrimental for liposome integrity, as freezing causes increase in the release of the drug and vesicle size after lyophilization. The use of cryoprotectant may improve the resistance of nano-particles to the damaging effect of freeze drying. In our study, it was found that no significant differences in particle size and percentage of drug release were existed when sucrose was added to liposomes at 0.5:1, 1:1 and 2:1 M ratios (sucrose: lipid).

3.5. Cytotoxicity assay

MTT assay is a method for assessing cell metabolic activity. In viable cells, yellow tetrazolium salt MTT converts into a purple colored formazan product by succinate dehydrogenase of mitochondria. The resulting intracellular purple formazan can be solubilized and quantified by spectrophotometrically. When cells die, they lose the ability to convert MTT into formazan, therefore color formation serves as a useful and convenient marker of only the viable cells [24,25]. The different concentrations for MTT assay were selected according to our preliminary studies and literatures. The results from MTT viability tests are presented in Fig. 4A–E and in the form of IC_{50} in Table 6. In HT-29, Caco-2 and HeLa cells, folate-liposomal 5FU exhibited significant higher toxicity as compared to 5FU and liposomal 5FU (Fig. 4A–C). Moreover, there were no differences in cytotoxicity between 5FU and liposomal 5FU (non-targeted) on cancer cells. As shown in Fig. 4D, targeted liposomes could not prove to be more effective against the MCF-7 cells due to their FR-negative feature (Fig. 4D). As it could be seen from Fig. 4E, cytotoxicity of liposomal 5FU and folate-liposomal 5FU in fibroblast cells was lower than free drug, because of lower FRs expression level in normal cells and their over expressing in tumor cells. Based on the results of MTT, HT-29 and HeLa cell lines were selected for further evaluations.

3.6. Cytotoxicity pathway evaluation in HT-29 cells exposed to IC_{50} concentrations of 5FU and folate-liposomal 5FU

As displayed in Fig. 5A, after exposing HT-29 cells to 5FU and folate-liposomal 5FU for 1, 3 and 48 h, 5FU exhibited a higher intracellular ROS generation. To determine the influence of 5FU and folate-liposomal 5FU on the mitochondrial membrane potential ($\Delta\Psi_m$),

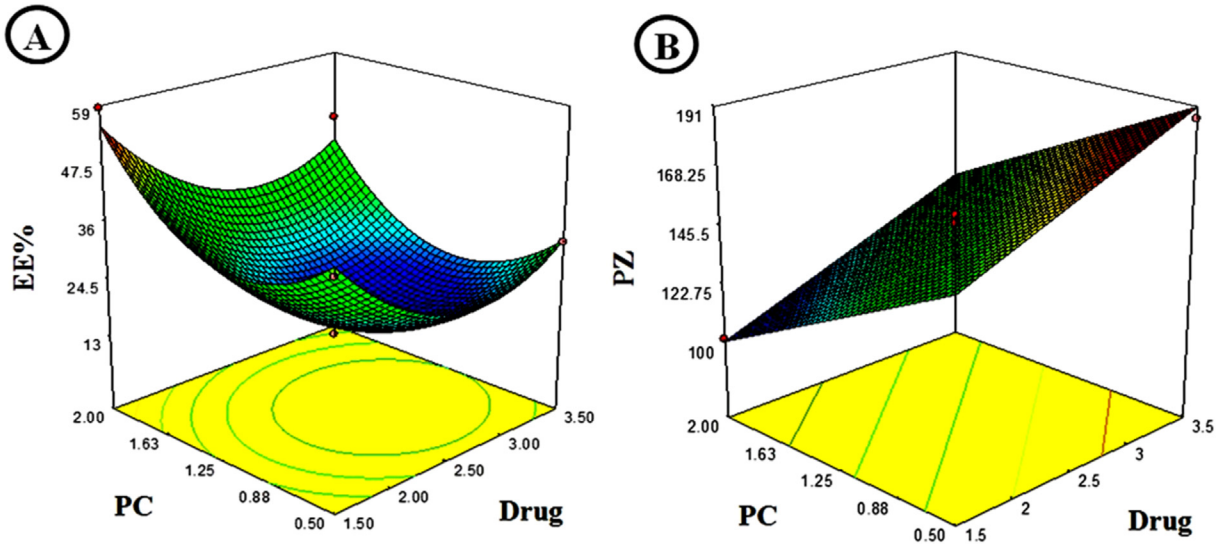

Fig. 2. Response surface plots for a) EE% and b) size of liposomes obtained from optimum formulation.

Table 5
Predicted and experimental values of the responses obtained at optimum conditions.

Independent variable		Optimized amount	Dependent variable		Predicted amount	Observed amount	Prediction error (%)
X_1	Drug	1.5	Y_1	EE%	55.0121	60.79	10.51
X_2	PC	2	Y_2	Size	100.772	104.8	3.98

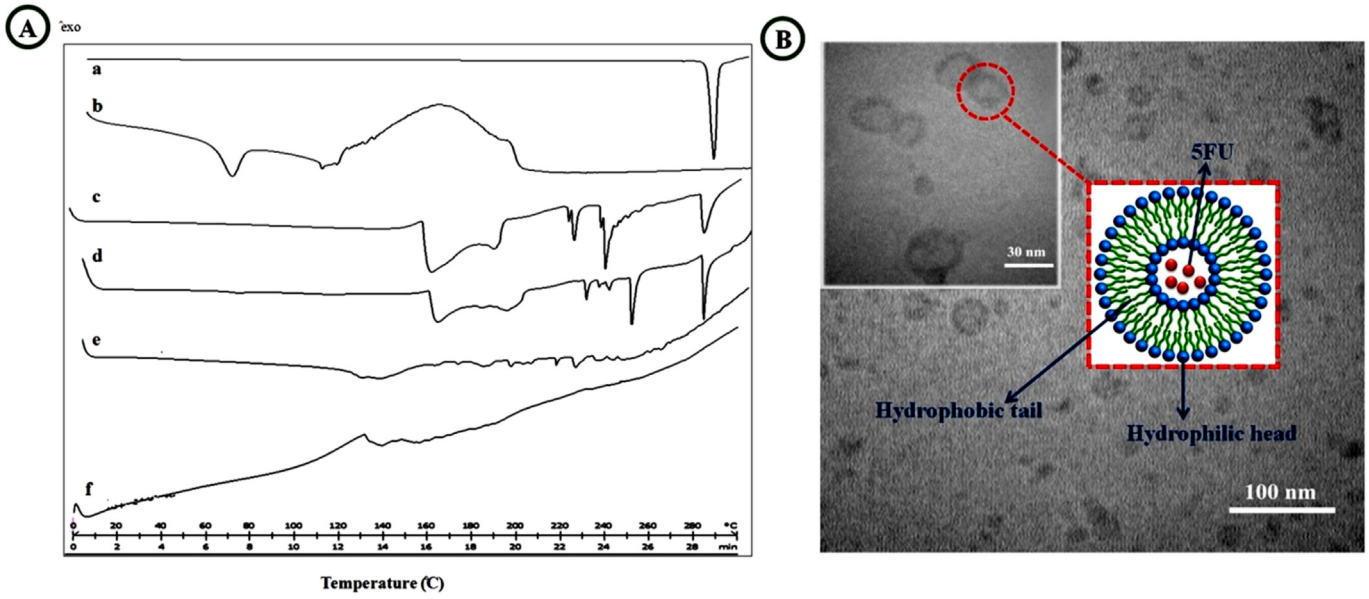

Fig. 3. A) DSC thermograms of (a) 5FU, (b) cholesterol, (c) PC, (d) physical mixture of 5FU/cholesterol/PC, (e) 5FU loaded liposome and (f) freeze dried powder of 5FU loaded liposome and B) TEM image of 5FU loaded liposome.

MitoLight dye (lipophilic cation) was employed. In healthy cells, this dye accumulates in the mitochondria and emits a red fluorescence, while in apoptotic cells where mitochondrial membrane potential has been declined, the dye distributes in a monomeric form in the cytosol and gives off a green fluorescence [32]. According to Fig. 5B, the $\Delta\Psi_m$ of HT-29 cells treated with free drug and targeted drug liposome were 0.06% and 0.60%, respectively. $\Delta\Psi_m$ collapsing of mitochondria is often leads to the opening of transition pores by which cytochrome *c* leaves the mitochondria. In this study, cytochrome *c* release was detected as a marker of apoptosis, due to the mitochondrial membrane permeabilization during apoptosis. In the HT-29 cells, high cytochrome *c* release was observed in the targeted drug liposome group (Fig. 5C). Fig. 5D displays the activities of caspase3/7 in the HT-29 cells. In HT-29 cells, folate-liposomal 5FU induced higher level of activated caspases compared to free drug which is in accordance with cytochrome *c* release manner. As shown in Fig. 5E, apoptosis rate is higher for targeted drug.

3.7. Cytotoxicity pathway evaluation in HeLa cells exposed to IC_{50} concentrations of 5FU and folate-liposomal 5FU

As shown in Fig. 6A, the generation of ROS in HeLa cells after incubating with targeted drug liposome, was significantly enhanced.

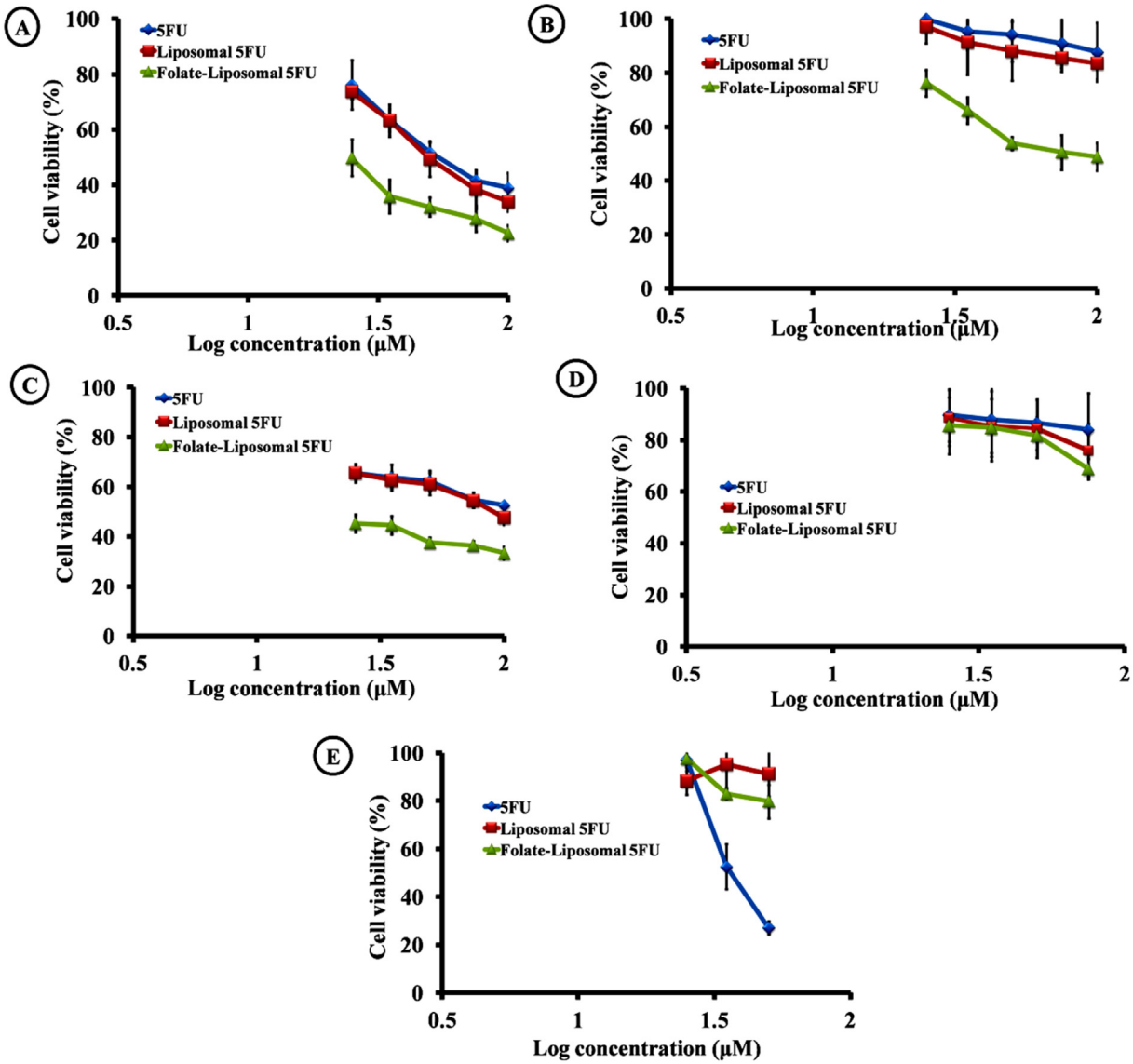

Fig. 4. Cytotoxicity of different formulations of 5FU on A) HT-29, B) Caco-2, C) HeLa, D) MCF-7 and E) fibroblast by MTT method in DMEM medium at 37 °C for 48 h. Data were given as mean ± SD ($n = 3$).

Table 6
IC_{50} values (μM) for 5FU, Liposomal 5FU and folate-liposomal 5FU on various cells.

Formulation	HT-29	Caco-2	HeLa	MCF-7	Fibroblast
5FU	58.88	–	134.896	–	38.01
Liposomal 5FU	53.70	–	97.72	933.25	575.44
Folate-liposomal 5FU	19.95	79.43282	15.49	323.593	147.91

Furthermore, after treatment with 5FU and folate- liposomal 5FU for 48 h, the $\Delta\Psi_m$ collapse in exposed cells was 1.06% and 0.44%, respectively (Fig. 6B). In these cells, 5FU led to release of higher amount of cytochrome *c* than folate-liposomal 5FU (Fig. 6C). As shown in Fig. 6D, 5FU induced higher caspase 3/7 activity than targeted drug liposome and when HeLa cells treated with 5FU and folate-liposomal 5FU, apoptosis was induced 11.06% and 9.59%, respectively (Fig. 6E).

3.8. *In vivo anti-tumor activity and histopathological study*

Schematic representation of the experimental design *in vivo* is shown in Fig. 7A. Folate-liposomal 5FU exhibited a considerable tumor inhibition *in vivo* compared with free drug and the control groups ($p < 0.05$) (Fig. 7B). As shown in Fig. 7C, the tumor size of targeted liposome treated group was also smaller than those of the free 5FU treated and control group. Moreover, according to Fig. 7D, in comparison with control group, the folate-liposomal 5FU treated group exhibited lower cell density in the tumor tissue.

4. Discussion

In the current study, for preparation of PC liposomes, 1 mol of cholesterol was used; while, in the previous study 2 mol cholesterol employed for DPPC liposome preparation since by enhancement of the amount of cholesterol, better EE% for DPPC liposomes been achieved [23].

In this study, we found that by increasing the amount of PC, EE% was enhanced. The present findings are in agreed with the previous reports that 5FU entrapment efficiency can be increased by increasing the amount of phospholipids used [33,34]. The trapping efficiency of 5FU is low since it is highly water-soluble that rendering it non-interacting with the bilayer lipids [35]. It was reported that by increasing the ratio of phospholipids of liposomes, they become more rigid with

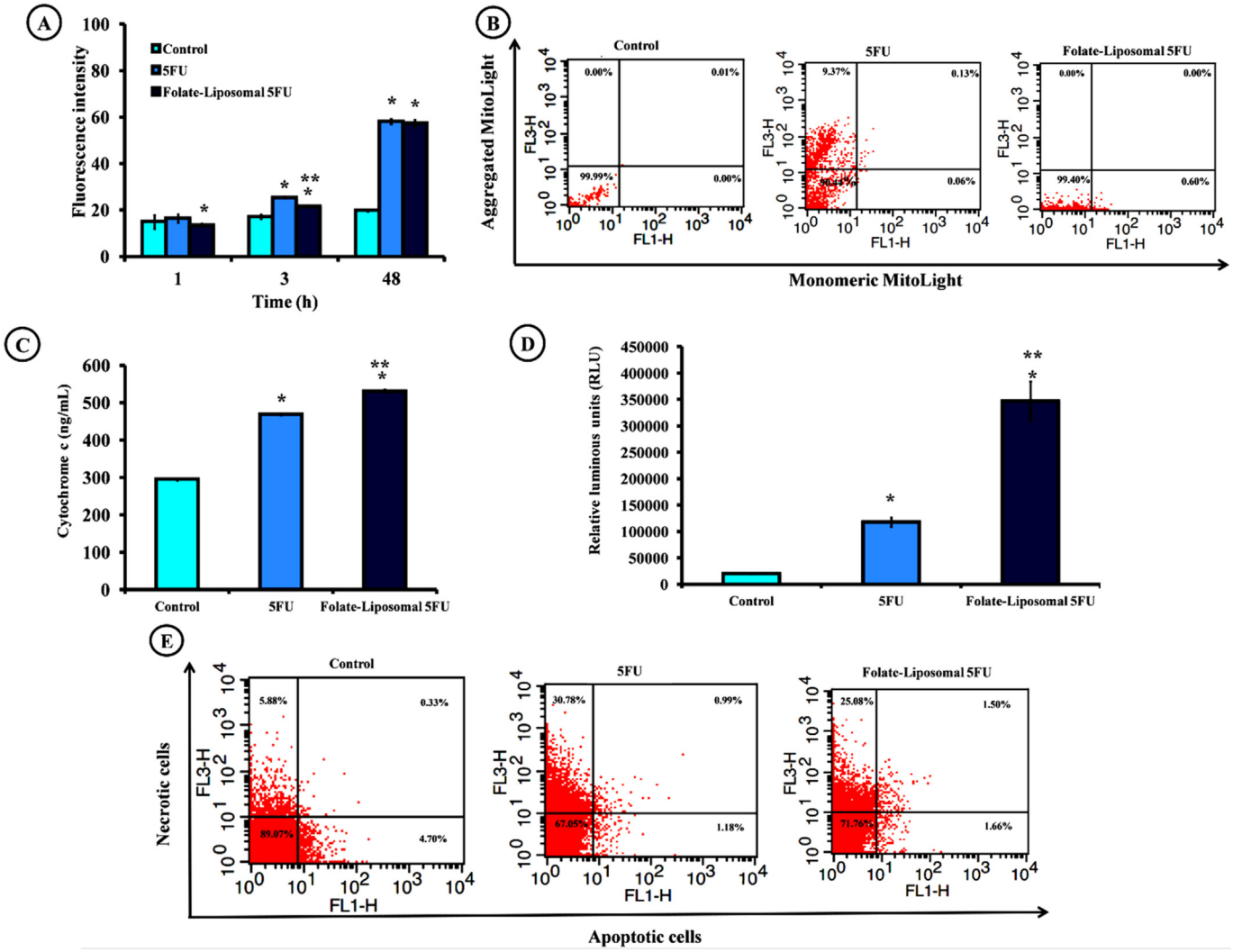

Fig. 5. The intracellular effects of free 5FU and folate-liposomal 5FU in HT-29 cells A) ROS production, B) $\Delta\Psi_m$ collapse C) cytochrome *c* release, D) caspase activity, E) apoptosis and necrosis rate. Cells were exposed to the IC_{50} of free 5FU and folate-liposomal 5FU for 48 h at 37 °C. Data were given as mean ± SD ($n = 3$).
*: Significant different with control.
**: Significant different with free drug.

having ability to retain more drug [36]. On the other hand, as shown in Fig. 2, the EE% decreased by increasing the amount of 5FU. It is believed that increasing of drug encapsulation is dependent on the inner space capacity of liposomes as well as the amount of free drug in the medium. At very high concentrations of drug, the surface attached drug percentage become negligible therefore any additional enhancement in the amount of drug would not lead to increasing in drug encapsulation [19]. We also observed that by enhancement the amount of drug, particle size of liposomes was increased, although by increasing amount of PC, it was decreased (Fig. 2). Incorporating of higher amounts of drug in the liposome may be attributed to the enlargement of liposome core. In addition, by increasing the amount of PC, liposomes turn to a condensed mass which this mass can result in the reduction of the size.

In our previous work, enhancement in the amount of DPPC led to an increase in particle size but additional increasing in the amount of lipid has decreased the particle size of liposomes. In addition, enhancement in the amount of drug increased the particle size to middle zone and after that the descending trend was achieved. In our previous study, EE % and particle size of DPPC liposome were 39.71% and 174 nm, respectively. However, in the current work, we prepared liposomes from PC with EE% of 60.79 and particle size of 104.8 nm. As can be seen, smaller liposome size and higher encapsulation efficiency of the drug were observed for PC liposome (present work) than DPPC liposome [23].

In this study, HT-29 and Caco-2 cell lines were selected as colon cancer cells and in order to examine the efficiency of targeted drug liposome, the cytotoxicity was also tested in the folate receptor (FR)-positive HeLa cells [8] and FR-negative MCF-7 cells [6]. To further confirm the safety of new formulation, fibroblast cells were employed as normal cells. In HT-29 and Caco-2 cells, folate-liposomal 5FU showed significant higher toxicity as compared with 5FU and liposomal 5FU. As it could be seen from Fig. 4A and B, there were no differences in cytotoxicity between 5FU and liposomal 5FU (non-targeted) on cancer cells. Similar result was observed in the study of Roger et al. (2012). They also found that cytotoxicity of paclitaxel loaded in FA targeted nano-particles was more than the free drug [37]. Also, in HeLa cells targeted liposome had significantly superior cytotoxic effects than free 5FU and liposomal 5FU. The drug-loaded liposomes (non-targeted) had similar activity to 5FU in inhibiting the growth of HeLa cells (Fig. 4C). Zhang et al. (2010) indicated that overexpression of FRs on the HeLa cells extensively improved the uptake of the targeted nano-particles *via* FR-mediated endocytosis and therefore resulted in higher cytotoxicity [38]. The interesting finding was that targeted drug liposome did not prove to be more effective against the MCF-7 cells mainly because of

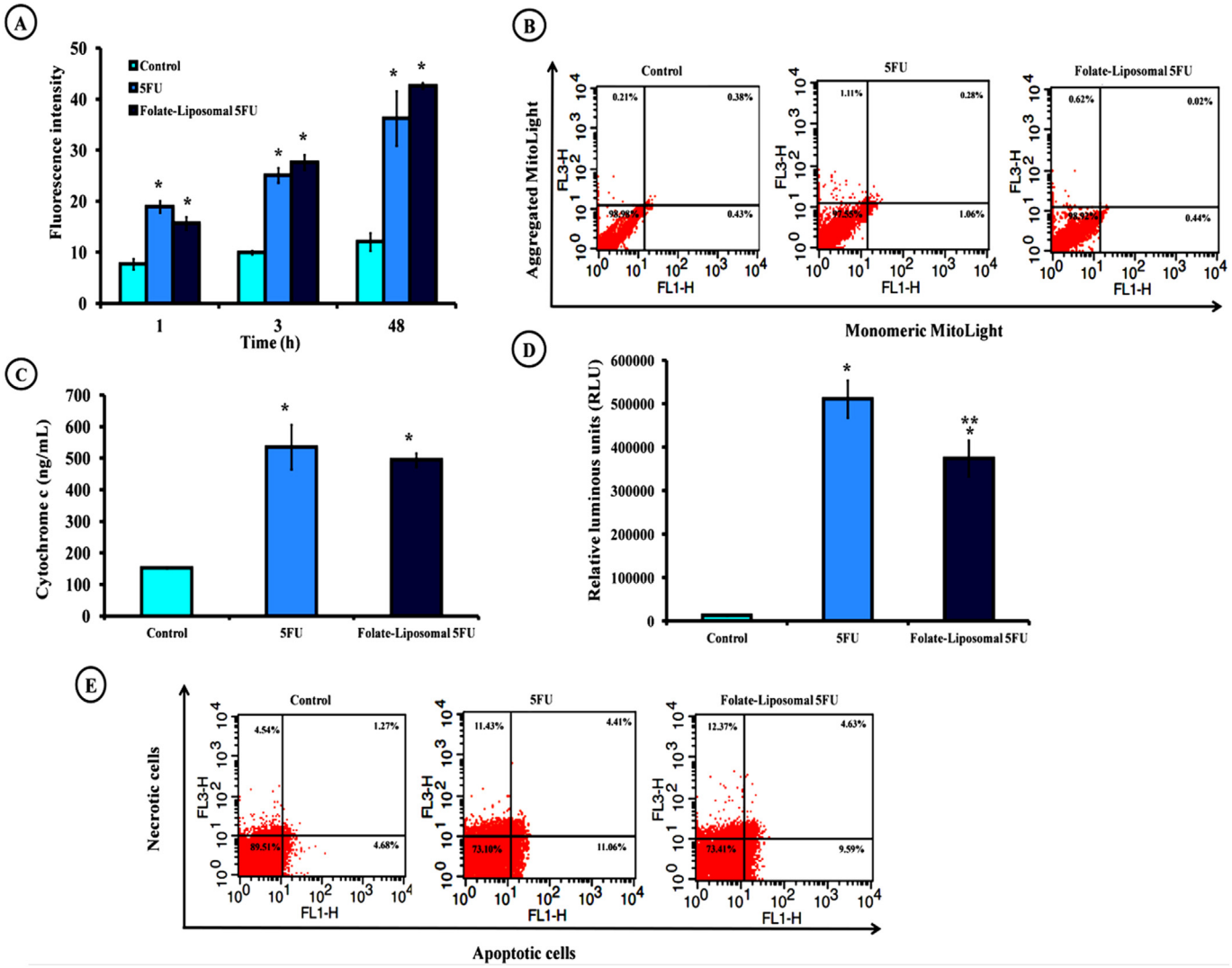

Fig. 6. The intracellular effects of free 5FU and folate-liposomal 5FU in HeLa cells A) ROS production, B) $\Delta\Psi_m$ collapse C) cytochrome *c* release, D) caspase activity, E) apoptosis and necrosis rate. Cells were exposed to the IC_{50} of free 5FU and folate-liposomal 5FU for 48 h at 37 °C. Data were given as mean ± SD ($n = 3$).
*: Significant different with control
**: Significant different with free drug.

their FR-negative feature (Fig. 4D). These findings confirm the results of Banu et al. (2015), which observed that the efficacy of doxorubicin loaded in FA targeted nano-particles on MDA-MB-231 cells was more than MCF-7 cells. They suggested that it may be attributed to the low expression of FRs on the surface of MCF-7 cells [6]. Another important finding was that cytotoxicity of liposomal 5FU and folate-liposomal 5FU in fibroblast cells was lower than free drug, probably due to lower FRs expression level in normal cells and their over expressing within the tumor cells (Fig. 4E). These findings suggest that the cytotoxic activity of targeted liposomes is particularly dependent on the cell type. This observation is in agreement with the findings of Lv et al. (2017). They implied that capsaicin loaded FA targeted nano-particle had no effect on normal cells, due to lake of any FRs on the surface of normal cells [39].

It is well know that cancer cells have higher levels of ROS compared with normal cells [40] that play a role in activating of cell apoptotic and necrotic signaling induced by anticancer agents. Since 5FU may trigger oxidative stress and ROS production, we further assessed the necrotic and apoptotic cell death induced by treatment of 5FU in HT-29 and HeLa cells. After exposing HT-29 cells to 5FU and folate-liposomal 5FU, free drug showed a higher intracellular ROS generation. Previous studies also demonstrated that 5FU remarkably increased ROS production in cancer cells [41]. However, this finding is contrary to the results of Laha et al. (2015) that showed FA targeted nano-particle enhanced ROS production in cancer cells [42]. Mitochondria were proposed to be the main source for intercellular ROS production and electron transport chain defects resulted from toxicants and drugs considered as a site for leakage of ROS [43]. Therefore in our study we examined whether this ROS overproduction could be due to the mitochondrial dysfunction. The results showed that folate-liposomal 5FU caused a disruption in the mitochondrial membrane potential. These results indicate that the source for ROS generation in cells treated with 5FU is different from folate-liposomal 5FU and probably resides outside the mitochondrion. On the other hands, $\Delta\Psi_m$ collapsing of mitochondria causes the release of cytochrome *c* from mitochondria to cytosol. According to the findings, after exposing HT-29 cells to targeted drug liposome, high cytochrome *c* release was observed. These results suggest the activation of mitochondria-mediated apoptosis pathway especially for targeted drug. Targeted liposomes triggered apoptotic pathway in cancer cells through the collapse of $\Delta\psi_m$ and release of cytochrome *c* from mitochondria [44]. Pagliara et al. (2016) showed that after exposing of cancer cells to 5FU, a significant release of cytochrome *c* was observed [45]. Determination of the activity of executive caspases subsequently confirms the above maintained results. In the HT-29 cells, higher level of activity

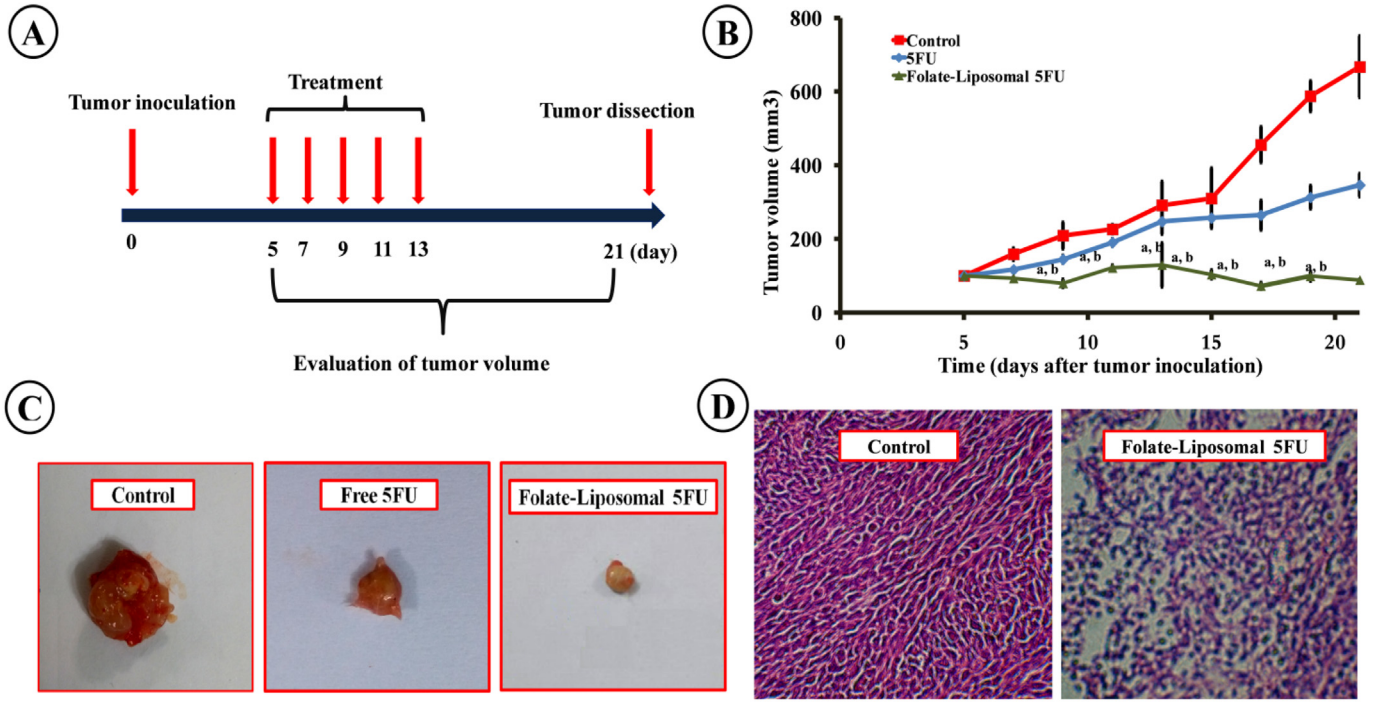

Fig. 7. Evaluation of *In vivo* anticancer activity of free 5FU and folate-liposomal 5FU: A) schematic representation of the experimental design, B) tumor volume, C) images of solid tumor and D) histopathology images of tumor sections with H&E staining of different experimental groups. Data were given as mean ± SD (n = 3).
a: Significant different with control.
b: Significant different with free drug.

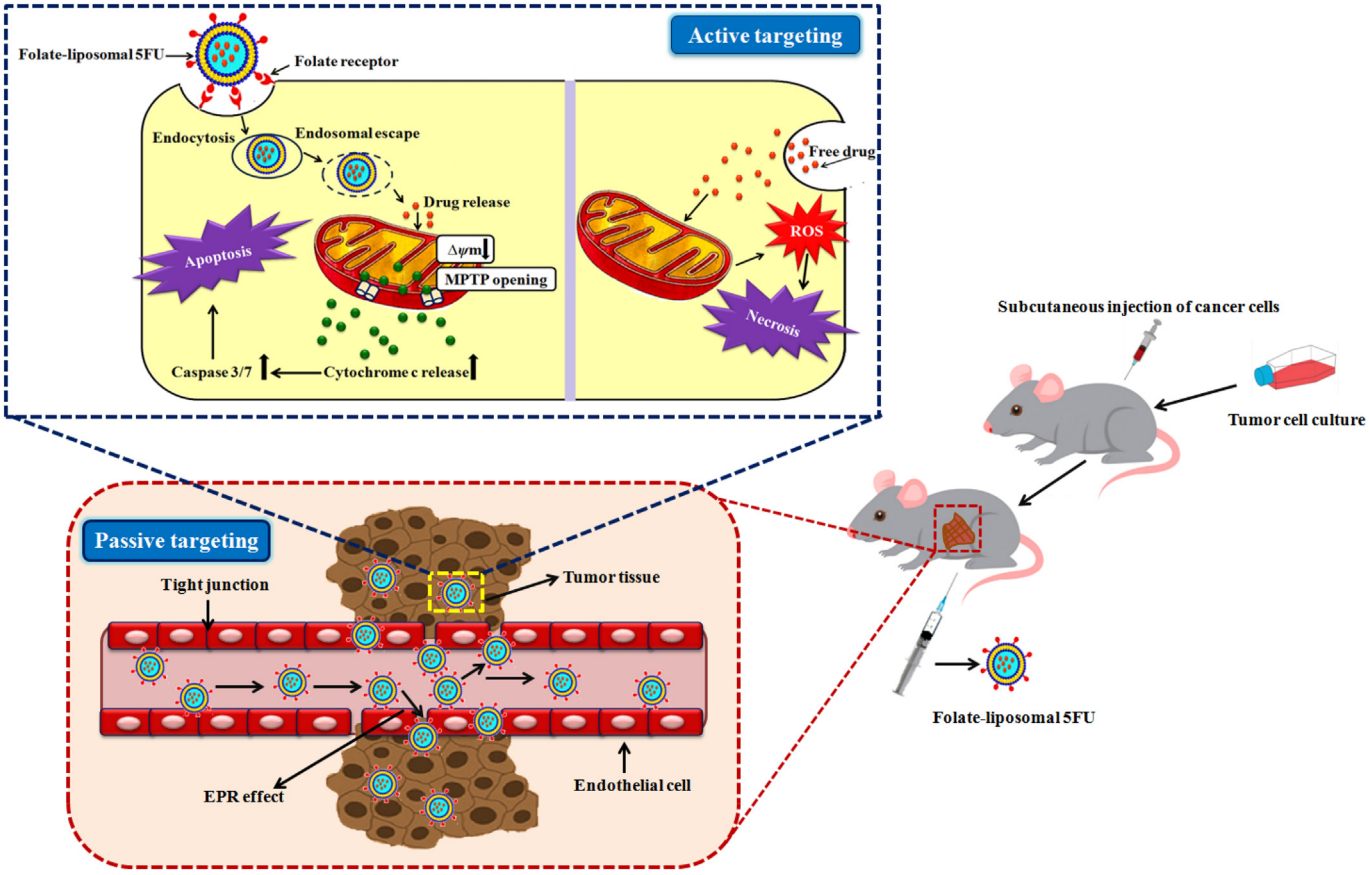

Fig. 8. Schematic representation of antitumor activity of folate-liposomal 5FU in cancer cells.

of caspases was observed in the targeted drug liposome group. Lower level of ROS for targeted drug gives rise to lower rate of necrotic than apoptotic cell death [46]. In cancer therapy induction of cell death by anticancer agents would be more advantages to occur through the apoptotic pathway, since necrotic cell death contributes to release of massive inflammatory mediators from died cells [47]. As shown in Fig. 5E, HT-29 cells after treatment with 5FU and folate-liposomal 5FU, apoptosis induction was 1.18% and 1.66%, respectively. The targeted 5FU liposomes exhibited higher apoptosis-inducing capacity compared to free 5FU. These results demonstrate that apoptosis in HT-29 cells could be enhanced by targeting 5FU liposomes. These data confirms previous studies in which FA targeted nano-particles triggered apoptosis pathway by over production of ROS and collapse of mitochondrial membrane potential [39,48].

In contrast to HT-29 cells, the generation of ROS in HeLa cells after treating with targeted drug liposome, was significantly enhanced (Fig. 6A). Increase in ROS generation probably indicates that the targeted drug liposome improved accumulation of drug in the cancer cell for triggering the cell death mainly through the necrosis. In addition, after treatment of HeLa cells with 5FU and folate-liposomal 5FU, the $\Delta\Psi_m$ collapse determined 1.06% and 0.44%, respectively. The finding demonstrated that free drug produced the most significant disruption of negatively charged mitochondrial membranes and triggered the highest depolarization. 5FU led to release of higher amount of cytochrome *c* than folate-liposomal 5FU in HeLa cells. The consequence of these changes suggests that 5FU alone may signal the cells to start the apoptotic process more effectively than folate-liposomal 5FU. As expected, the results implied that the free drug activated mitochondrial apoptosis pathway more potently. Moreover, 5FU induced higher caspase 3/7 activity than targeted drug liposome and apoptosis rate induced by 5FU was higher than folate-liposomal 5FU. According to the results, cell death by targeted liposomes, moves further towards necrosis. These results are consistent with the study of Kaehler et al. (2014). They indicated that 5FU promote apoptosis in HeLa cell [49]. However, Juang et al. (2016) reported that targeted liposomes triggered apoptosis pathway in HeLa cells by collapse of mitochondrial membrane potential and increase in the activity of caspases [50]. Ji et al. (2015) also implied that FA targeted nano-particles induced higher apoptosis in HeLa cells [51]. However, it should be noted that in comparison with free drug, 5FU loaded liposomes exhibited extra rate of apoptosis with lower IC_{50} (15.49 μM compared to 134.89 μM). This reduction in dose or concentration (with retained efficacy) certainly decreases the adverse effects of drug and chemotherapy and will improve the adherence of treatment in patients.

The mechanism we observed for cell death in the current work was different from the previous study on HT-29 and HeLa cells. In the previous work, folate targeted DPPC liposome induced necrosis pathway on HT-29 and apoptosis on HeLa cells [23].

The proposed mechanism of action of 5FU and folate-liposomal 5FU is shown in Fig. 8.

As shown in Fig. 7A, folate-liposomal 5FU exhibited a considerable tumor inhibition *in vivo* compared with free drug and the control groups ($p < 0.05$). The tumor size of targeted liposome treated group was also smaller than those of the free 5FU treated and control group (Fig. 7B). Furthermore, there was no considerable weight loss or changes in the activity and feeding between the treated and control groups (data not shown).

In the current study, PC liposome showed better tumor inhibition than previous work (DPPC liposome) (80.71 cm^3 *vs* 169 cm^3) [23].

The enhanced anti-tumor efficacy of folate-liposomal 5FU might be associated with permeability and retention (EPR) effect. According to the previous study, 100 to 200 nm NPs can internalize in solid tumors due to EPR effects through the defected blood vessels and lymphatic drainage. In current study, the mean particle size of nanoparticles was around to be 104 nm, which are appropriate for accumulation into cancer cells. In addition, significant reduction in tumor volume was probably due to the folic acid present in the surface of liposomes which increased anticancer efficacy in cancer cells. On the other hands, according to our *in vitro* results, inhibition of tumor cells may be related to apoptosis-inducing effect of targeted drug liposome. Based on our results and previous reports, it seems that folate targeted liposomes can inhibit tumor growth through passive and active targeting as well as induction of apoptosis in tumor tissue. The proposed mechanism of antitumor activity of folate-liposomal 5FU in cancer cells is presented schematically in Fig. 8.

Also, as shown in Fig. 7D, in comparison with control group, the folate-liposomal 5FU treated group exhibited lower cell density in tumor tissue. These findings revealed that targeted liposomes can be employed as an ideal nanoplatform for the delivery of drugs for more effective cancer treatment. More detailed of tissue distribution and kinetic parameter values are under further study.

5. Conclusion

In the present study, the effect of different amounts of 5FU and PC on the preparing of optimal 5FU liposomes was investigated. According to the results, these amounts were detected as effective variables on particle size and encapsulation efficiency for liposome preparation. The optimum conditions for the preparation of 5FU liposomes were the ratio of PC: cholesterol (2:1) and amount of drug (1.5 mg). Under these conditions, the EE% and particle size were 60.79 and 104.8 respectively. DSC analysis showed that drug was in an amorphous state in the formulation and liposomes were spherical as demonstrated by TEM. The remarkable results of cytotoxicity evaluations in HT-29 cells showed that compared to free 5FU, folate-liposomal 5FU induced significant higher apoptosis rate, represented by lower production of ROS, decreased $\Delta\Psi_m$, higher release of cytochrome *c* and caspase activity in concentrations much lower than 5FU. However, in HeLa cells, targeted liposomes caused death cells particularly *via* activating of ROS induced necrosis pathway. In addition, folate-liposomal 5FU exhibited superior *in vivo* antitumor activity.

Acknowledgment

The work was financially supported by Nanotechnology Research Center, Ahvaz Jundishapur University of Medical Sciences, Ahvaz, Iran (grant No. 111) and Iran National Science Foundation (grant No. INSF-93032941).

Conflict of interest

The authors declare no conflict of interest.

References

[1] V.R. Sinha, B.R. Mittal, K.K. Bhutani, R. Kumria, Colonic drug delivery of 5-fluorouracil: an in vitro evaluation, Int. J. Pharm. 269 (2004) 101–108.
[2] W. He, Q. Du, D.Y. Cao, B. Xiang, L.F. Fan, Study on colon-specific pectin/ethylcellulose film-coated 5-fluorouracil pellets in rats, Int. J. Pharm. 348 (2008) 35–45.
[3] W. Sun, N. Zhang, A. Li, W. Zou, W. Xu, Preparation and evaluation of N(3)-O-toluyl-fluorouracil-loaded liposomes, Int. J. Pharm. 353 (2008) 243–250.
[4] Y.S. Krishnaiah, V. Satyanarayana, B. Dinesh Kumar, R.S. Karthikeyan, P. Bhaskar, In vivo pharmacokinetics in human volunteers: oral administered guar gum-based colon-targeted 5-fluorouracil tablets, Eur. J. Pharm. Sci. 19 (2003) 355–362.
[5] Y.S. Krishnaiah, V. Satyanarayana, B. Dinesh Kumar, R.S. Karthikeyan, In vitro drug release studies on guar gum-based colon targeted oral drug delivery systems of 5-fluorouracil, Eur. J. Pharm. Sci. 16 (2002) 185–192.
[6] H. Banu, D.K. Sethi, A. Edgar, A. Sheriff, N. Rayees, N. Renuka, S.M. Faheem, K. Premkumar, G. Vasanthakumar, Doxorubicin loaded polymeric gold nanoparticles targeted to human folate receptor upon laser photothermal therapy potentiates chemotherapy in breast cancer cell lines, J. Photochem. Photobiol. B 149 (2015) 116–128.
[7] H. Shmeeda, L. Mak, D. Tzemach, P. Astrahan, M. Tarshish, A. Gabizon, Intracellular uptake and intracavitary targeting of folate-conjugated liposomes in a mouse lymphoma model with up-regulated folate receptors, Mol. Cancer Ther. 5 (2006) 818–824.
[8] Y. Gao, Z. Li, X. Xie, C. Wang, J. You, F. Mo, B. Jin, J. Chen, J. Shao, H. Chen, L. Jia,

Dendrimeric anticancer prodrugs for targeted delivery of ursolic acid to folate receptor-expressing cancer cells: synthesis and biological evaluation, Eur. J. Pharm. Sci. 70 (2015) 55–63.
[9] A. Laouini, C. Jaafar-Maalej, S. Sfar, C. Charcosset, H. Fessi, Liposome preparation using a hollow fiber membrane contactor—application to spironolactone encapsulation, Int. J. Pharm. 415 (2011) 53–61.
[10] G. Yang, Y. Zhao, Y. Zhang, B. Dang, Y. Liu, N. Feng, Enhanced oral bioavailability of silymarin using liposomes containing a bile salt: preparation by supercritical fluid technology and evaluation in vitro and in vivo, Int. J. Nanomedicine 10 (2015) 6633–6644.
[11] M.J. Barea, M.J. Jenkins, M.H. Gaber, R.H. Bridson, Evaluation of liposomes coated with a pH responsive polymer, Int. J. Pharm. 402 (2010) 89–94.
[12] Y. Yu, Y. Lu, R. Bo, Y. Huang, Y. Hu, J. Liu, Y. Wu, Y. Tao, D. Wang, The preparation of gypenosides liposomes and its effects on the peritoneal macrophages function in vitro, Int. J. Pharm. 460 (2014) 248–254.
[13] P. Toimil, R. Davina, J. Sabin, G. Prieto, F. Sarmiento, Influence of temperature on the colloidal stability of the F-DPPC and DPPC liposomes induced by lanthanum ions, J. Colloid Interface Sci. 367 (2012) 193–198.
[14] H. Liu, Y. Zhang, Y. Han, S. Zhao, L. Wang, Z. Zhang, J. Wang, J. Cheng, Characterization and cytotoxicity studies of DPPC:M2+ novel delivery system for cisplatin thermosensitivity liposome with improving loading efficiency, Colloids Surf. B: Biointerfaces 131 (2015) 12–20.
[15] X. Xu, M.A. Khan, D.J. Burgess, Predicting hydrophilic drug encapsulation inside unilamellar liposomes, Int. J. Pharm. 423 (2012) 410–418.
[16] C. Zeng, W. Jiang, M. Tan, X. Yang, C. He, W. Huang, J. Xing, Optimization of the process variables of tilianin-loaded composite phospholipid liposomes based on response surface-central composite design and pharmacokinetic study, Eur. J. Pharm. Sci. 85 (2016) 123–131.
[17] X. Luo, R. Guan, X. Chen, M. Tao, J. Ma, J. Zhao, Optimization on condition of epigallocatechin-3-gallate (EGCG) nanoliposomes by response surface methodology and cellular uptake studies in Caco-2 cells, Nanoscale Res. Lett. 9 (2014) 291.
[18] X. Zhao, J. Liu, Y. Hu, Y. Fan, D. Wang, J. Yuan, L. Xu, L. Cui, Z. Jing, Optimization on condition of glycyrrhetinic acid liposome by RSM and the research of its immunological activity, Int. J. Biol. Macromol. 51 (2012) 299–304.
[19] X. Xu, M.A. Khan, D.J. Burgess, A quality by design (QbD) case study on liposomes containing hydrophilic API: II. Screening of critical variables, and establishment of design space at laboratory scale, Int. J. Pharm. 423 (2012) 543–553.
[20] H. Xu, J. Paxton, J. Lim, Y. Li, Z. Wu, Development of a gradient high performance liquid chromatography assay for simultaneous analysis of hydrophilic gemcitabine and lipophilic curcumin using a central composite design and its application in liposome development, J. Pharm. Biomed. Anal. 98 (2014) 371–378.
[21] H. Xu, L. He, S. Nie, J. Guan, X. Zhang, X. Yang, W. Pan, Optimized preparation of vinpocetine proliposomes by a novel method and in vivo evaluation of its pharmacokinetics in New Zealand rabbits, J. Control. Release 140 (2009) 61–68.
[22] Y. Huang, C. Wu, Z. Liu, Y. Hu, C. Shi, Y. Yu, X. Zhao, C. Liu, J. Liu, Y. Wu, D. Wang, Optimization on preparation conditions of Rehmannia glutinosa polysaccharide liposome and its immunological activity, Carbohydr. Polym. 104 (2014) 118–126.
[23] S. Handali, E. Moghimipour, M. Rezaei, Z. Ramezani, M. Kouchak, M. Amini, K.A. Angali, S. Saremy, F.A. Dorkoosh, A novel 5-fluorouracil targeted delivery to colon cancer using folic acid conjugated liposomes, Biomed. Pharmacother. 108 (2018) 1259–1273.
[24] R.J. Lee, P.S. Low, Folate-mediated tumor cell targeting of liposome-entrapped doxorubicin in vitro, Biochim. Biophys. Acta 1233 (1995) 134–144.
[25] A. Waheed, Y. Bibi, S. Nisa, F.M. Chaudhary, S. Sahreen, M. Zia, Inhibition of human breast and colorectal cancer cells by Viburnum foetens L. extracts in vitro, Asian Pac. J. Trop. Dis. 3 (2013) 32–36.
[26] H. Wang, J.A. Joseph, Quantifying cellular oxidative stress by dichlorofluorescein assay using microplate reader, Free Radic. Biol. Med. 27 (1999) 612–616.
[27] M. Tabbakhian, J.A. Rogers, Interaction of insulin, cholesterol-derivatized mannan, and carboxymethyl chitin with liposomes: a differential scanning calorimetry study, Res. Pharm. Sci. 7 (2012) 43–50.
[28] A. Jain, S.K. Jain, In vitro and cell uptake studies for targeting of ligand anchored nanoparticles for colon tumors, Eur. J. Pharm. Sci. 35 (2008) 404–416.
[29] P. Singh, G. Tyagi, R. Mehrotra, A.K. Bakhshi, Thermal stability studies of 5-fluorouracil using diffuse reflectance infrared spectroscopy, Drug Test. Anal. 1 (2009) 240–244.
[30] J.S. Lee, G.S. Chae, T.K. An, G. Khang, S.H. Cho, H.B. Lee, Preparation of 5-fluorouracil-loaded poly(L-lactide-co-glycolide) wafer and evaluation ofin vitro release behavior, Macromol. Res. 11 (2003) 183–188.
[31] M. Nasr, M.K. Ghorab, A. Abdelazem, In vitro and in vivo evaluation of cubosomes containing 5-fluorouracil for liver targeting, Acta Pharm. Sin. B 5 (2015) 79–88.
[32] L. Sliwka, K. Wiktorska, P. Suchocki, M. Milczarek, S. Mielczarek, K. Lubelska, T. Cierpial, P. Lyzwa, P. Kielbasinski, A. Jaromin, A. Flis, Z. Chilmonczyk, The comparison of MTT and CVS assays for the assessment of anticancer agent interactions, PLoS One 11 (2016) e0155772.
[33] B. Elorza, M.A. Elorza, G. Frutos, J.R. Chantres, Characterization of 5-fluorouracil loaded liposomes prepared by reverse-phase evaporation or freezing-thawing extrusion methods: study of drug release, Biochim. Biophys. Acta 1153 (1993) 135–142.
[34] M. Glavas-Dodov, E. Fredro-Kumbaradzi, K. Goracinova, M. Simonoska, S. Calis, S. Trajkovic-Jolevska, A.A. Hincal, The effects of lyophilization on the stability of liposomes containing 5-FU, Int. J. Pharm. 291 (2005) 79–86.
[35] N. Kaiser, A. Kimpfler, U. Massing, A.M. Burger, H.H. Fiebig, M. Brandl, R. Schubert, 5-Fluorouracil in vesicular phospholipid gels for anticancer treatment: entrapment and release properties, Int. J. Pharm. 256 (2003) 123–131.
[36] A.N. Elmeshad, S.M. Mortazavi, M.R. Mozafari, Formulation and characterization of nanoliposomal 5-fluorouracil for cancer nanotherapy, J. Liposome Res. 24 (2014) 1–9.
[37] E. Roger, S. Kalscheuer, A. Kirtane, B.R. Guru, A.E. Grill, J. Whittum-Hudson, J. Panyam, Folic acid functionalized nanoparticles for enhanced oral drug delivery, Mol. Pharm. 9 (2012) 2103–2110.
[38] C. Zhang, L. Zhao, Y. Dong, X. Zhang, J. Lin, Z. Chen, Folate-mediated poly(3-hydroxybutyrate-co-3-hydroxyoctanoate) nanoparticles for targeting drug delivery, Eur. J. Pharm. Biopharm. 76 (2010) 10–16.
[39] L. Lv, Y.X. Zhuang, H.W. Zhang, N.N. Tian, W.Z. Dang, S.Y. Wu, Capsaicin-loaded folic acid-conjugated lipid nanoparticles for enhanced therapeutic efficacy in ovarian cancers, Biomed. Pharmacother. 91 (2017) 999–1005.
[40] H. Wu, S. Liu, J. Gong, J. Liu, Q. Zhang, X. Leng, N. Zhang, Y. Li, VCPA, a novel synthetic derivative of alpha-tocopheryl succinate, sensitizes human gastric cancer to doxorubicin-induced apoptosis via ROS-dependent mitochondrial dysfunction, Cancer Lett. 393 (2017) 22–32.
[41] M.P. Liu, M. Liao, C. Dai, J.F. Chen, C.J. Yang, M. Liu, Z.G. Chen, M.C. Yao, Sanguisorba officinalis L synergistically enhanced 5-fluorouracil cytotoxicity in colorectal cancer cells by promoting a reactive oxygen species-mediated, mitochondria-caspase-dependent apoptotic pathway, Sci. Rep. 6 (2016) 34245.
[42] D. Laha, A. Pramanik, S. Chattopadhyay, S.k. Dash, S. Roy, P. Pramanik, P. Karmakar, Folic acid modified copper oxide nanoparticles for targeted delivery in in vitro and in vivo systems, RSC Adv. 5 (2015) 68169–68178.
[43] V. Adam-Vizi, Production of reactive oxygen species in brain mitochondria: contribution by electron transport chain and non-electron transport chain sources, Antioxid. Redox Signal. 7 (2005) 1140–1149.
[44] X.X. Wang, Y.B. Li, H.J. Yao, R.J. Ju, Y. Zhang, R.J. Li, Y. Yu, L. Zhang, W.L. Lu, The use of mitochondrial targeting resveratrol liposomes modified with a dequalinium polyethylene glycol-distearoylphosphatidyl ethanolamine conjugate to induce apoptosis in resistant lung cancer cells, Biomaterials 32 (2011) 5673–5687.
[45] V. Pagliara, A. Saide, E. Mitidieri, B. Roberta d'Emmanuele di Villa, R. Sorrentino, G. Russo, A. Russo, 5-FU targets rpL3 to induce mitochondrial apoptosis via cystathionine-β-synthase in colon cancer cells lacking p53, Oncotarget 7 (2016) 50333–50348.
[46] M. Higuchi, T. Honda, R.J. Proske, E.T. Yeh, Regulation of reactive oxygen species-induced apoptosis and necrosis by caspase 3-like proteases, Oncogene 17 (1998) 2753–2760.
[47] P. Davidovich, C.J. Kearney, S.J. Martin, Inflammatory outcomes of apoptosis, necrosis and necroptosis, Biol. Chem. 395 (2014) 1163–1171.
[48] H. Jin, J. Pi, F. Yang, J. Jiang, X. Wang, H. Bai, M. Shao, L. Huang, H. Zhu, P. Yang, L. Li, T. Li, J. Cai, Z.W. Chen, Folate-chitosan nanoparticles loaded with ursolic acid confer anti-breast cancer activities in vitro and in vivo, Sci. Rep. 6 (2016) 30782.
[49] C. Kaehler, J. Isensee, T. Hucho, H. Lehrach, S. Krobitsch, 5-fluorouracil affects assembly of stress granules based on RNA incorporation, Nucleic Acids Res. 42 (2014) 6436–6447.
[50] V. Juang, H.-P. Lee, A.M.-Y. Lin, Y.-L. Lo, Cationic PEGylated liposomes incorporating an antimicrobial peptide tilapia hepcidin 2–3: an adjuvant of epirubicin to overcome multidrug resistance in cervical cancer cells, Int. J. Nanomedicine 11 (2016) 6047–6064.
[51] J. Ji, P. Zuo, Y.-L. Wang, Enhanced antiproliferative effect of carboplatin in cervical cancer cells utilizing folate-grafted polymeric nanoparticles, Nanoscale Res. Lett. 10 (2015) 453.